NANO LETTERS

2008
Vol. 8, No. 7
1830-1835

Supramolecular Discrimination of Carbon Nanotubes According to Their Helicity

Renaud Marquis,[†] Carla Greco,[†] Izabela Sadokierska,[†] Sergei Lebedkin,[‡] Manfred M. Kappes,[‡] Thierry Michel,[§] Laurent Alvarez,[§] Jean-Louis Sauvajol,[§] Stéphane Meunier,*[,†] and Charles Mioskowski[†,||]

Laboratoire de Synthèse Bio-Organique, CNRS-UMR7175/LC1, Institut Gilbert Laustriat, Faculté de Pharmacie, Université Louis Pasteur, 74 route du Rhin, 67401 Illkirch, France, Institut für Nanotechnologie, Forschungszentrum Karlsruhe, D-76021 Karlsruhe, Germany, and Laboratoire des Colloïdes, Verres et Nanomatériaux, CNRS-UMR5587, Université Montpellier II, 34095 Montpellier Cedex 5, France

Received January 31, 2008; Revised Manuscript Received April 29, 2008

ABSTRACT

Adsorption of specifically designed and geometrically constrained polyaromatic amphiphiles on single-walled carbon nanotubes (SWNTs) was found to be selective of the nanotube helicity angle. Starting from the same SWNT mixture, photoluminescence and resonant Raman spectroscopies show that a pentacenic-based amphiphile leads to the solubilization of armchair SWNTs and that a quaterrylene-based amphiphile leads to the solubilization of zigzag SWNTs. The results were predicted by the design of the two amphiphiles and are consistent with a supramolecular recognition of the nanotube graphene-type atomic structure by the aromatic part of the molecules through optimized $\pi-\pi$-stacking interactions.

Single-walled carbon nanotubes (SWNTs) are typically grown as mixtures of tubes with variable diameter and random helicities of their graphene-type lattice. Each type of SWNT is structurally defined by two integers (n,m; Figure 1a). Because the physical and chemical properties of SWNTs depend strongly on their structure, the separation of crude samples is one of the foremost technological hurdles for their investigation and for future development of nanotube-based technologies. The ideal separation method should be of the highest degree of selectivity in terms of SWNT indices (n,m) and also should be nondestructive for the selected tubes. So far, SWNTs have been sorted according to their electronic properties, allowing the theoretical exclusion of one-third (metallic tubes, $n - m = 3k$, where k is an integer) or two-thirds (semiconducting tubes, $n - m \neq 3k$, where k is an integer) of the tube population contained in the initial mixtures.[1–3] The corresponding techniques include selective chemical functionalization or oxidation; this involves a chemical attachment onto SWNTs and therefore the change of the electronic structure of the nanotubes.[4–7] Nondestructive enrichment in metallic tubes was achieved using dielectrophoresis[8,9] and density gradient assisted separation,[10,11] sometimes with the concomitant selection of a precise diameter or of an average length. Selections in SWNT diameter have also been possible by the tuning of the growth processes[12–14] or directly from as-produced mixtures (usually by the use of a size-exclusion based separation method) yielding mixtures of tubes with random helicities. The most attractive and potent approach is by DNA assisted dispersion[15–17] or polymer wrapping,[18] where the selectivity arises from the stability of the SWNT−DNA or the SWNT−polymer complex in solutions.

Very recently R. J. Nicholas reported the first efficient selection of armchair SWNTs (indices $n = m$, helicity of 30°, Figure 1a,b) from as-produced mixtures.[19,20] The authors studied the solubilizing properties of a collection of aromatic polymers for SWNTs in organic solvents. The regular wrapping of some polymers around the tubes have induced the selective solubilization of close-to-armchair tubes. However, because the origin of the selections are rather ill-defined, it seems difficult to tune the flexible polymers structure in order to orientate the selection toward SWNT subsets presenting other helicities.

* To whom correspondence should be addressed. E-mail: meunier@bioorga.u-strasbg.fr.
† Université Louis Pasteur.
‡ Forschunszentrum Karlsruhe.
§ Université Montpellier II
|| Deceased June 2nd, 2007. This article is dedicated to the memory of Charles Mioskowski who initiated this work.

10.1021/nl0803141 CCC: $40.75
Published on Web 06/10/2008

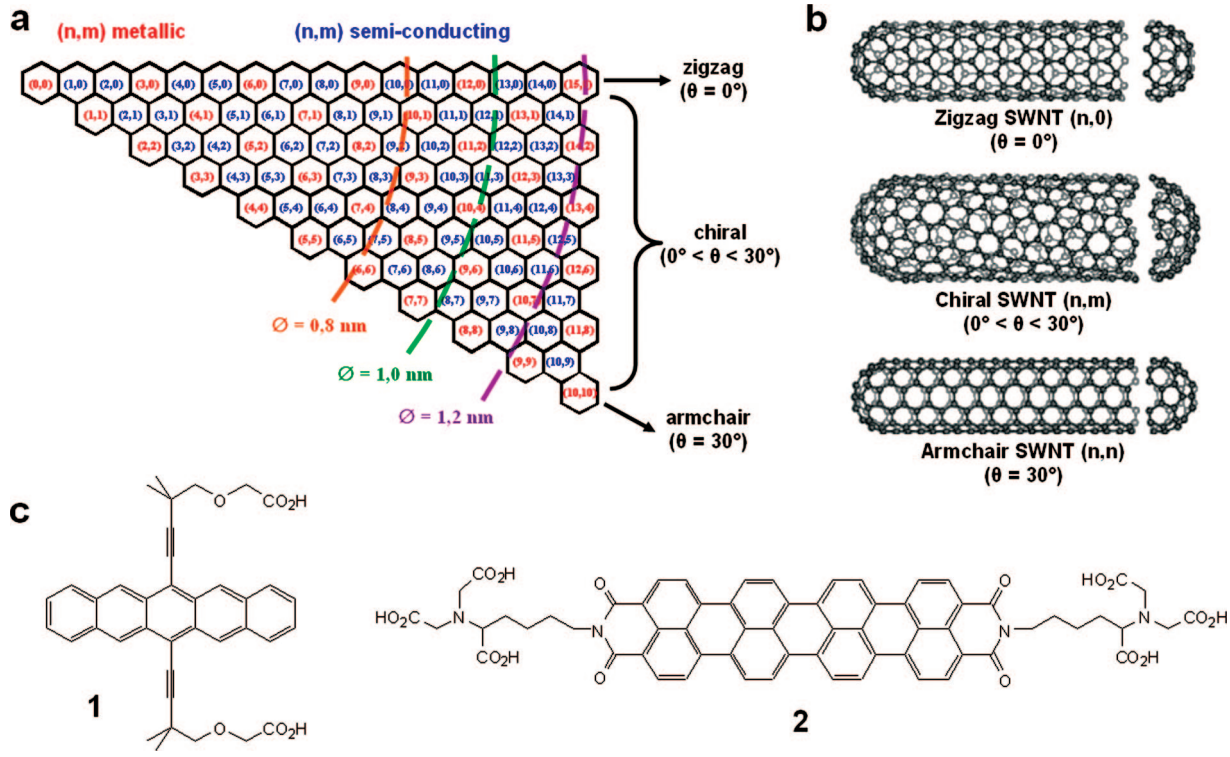

Figure 1. Structures of SWNTs and of the two aromatic amphiphiles synthesized for the selective solubilization of SWNTs. (a) Graphene sheet segment showing indexed lattice points, known as a Hamada plot. Nanotubes designated (*n*,*m*) are obtained by rolling the sheet from (0,0) to (*n*,*m*); their diameter is determined by the distance between these two points. On a helicity stand point, SWNTs are distributed in three categories: the "armchair" tubes with (*n*,*n*) coordinates (helicity angle equal to 30°), the "zigzag" tubes with (*n*,0) coordinates (helicity angle equal to 0°), and the chiral tubes with other (*n*,*m*) coordinates ($n \neq m \neq 0$, helicity angle ranging from 0° to 30°). (b) Idealized structures of a zigzag, a chiral, and an armchair SWNT. (c) Structures of the aromatic amphiphiles; considering the structure of their aromatic bodies and the atomic structure of SWNTs, we expect compound **1** to adsorb preferentially at the surface of armchair SWNTs and compound **2** to adsorb at the surface of zigzag nanotubes.

In other very recent reports by N. Komatsu, the use of precisely designed rigid small molecules allowed for the first time the selective solubilization of right and left handed SWNTs.[21,22] These chiral zinc(II) diporphyrins specifically interacted through $\pi-\pi$-stacking and charge transfer interactions with the helical structures of chiral nanotubes contained in an as-produced CoMoCAT sample. However, there were no notable discriminations based on the helicity angle, as the (*n*,*m*) population was virtually unchanged after the solubilizing treatment.

As a starting point for our studies, we wished to design several small amphiphiles which should be able, from an as-produced mixture of nanotubes, to extract and solubilize in water specific SWNT subsets with (*n*,*m*) selectivities based on the nanotube helicity angle (Figure 1a). Herein are presented the results allowing us to validate this concept by using the selectivity of $\pi-\pi$-stacking interactions.

In order to conceive amphiphiles that will allow the specific solubilization of nanotubes of different helicities from a starting SWNT mixture, we anticipated that geometrically constrained polyaromatic molecules should have selective $\pi-\pi$-stacking interactions with nanotubes, according to the best fit between the molecule and the tube graphene-type structure. Two amphiphiles were designed for the selective solubilization of armchair (Figure 1b, indice $m = n$, helicity of 30°) and zigzag tubes (Figure 1b, indice $m = 0$, helicity of 0°).

Amphiphile **1** (Figure 1c) contains a pentacenic moiety and two hydrophilic side chains that are negatively charged in basic aqueous media. This molecule is expected to adsorb to the armchair SWNT sidewalls in order to maximize the $\pi-\pi$-stacking interactions: simultaneous optimization of the effective contact area and of the atomic correlation with the carbon nanotube.[23–25] Amphiphile **2** (Figure 1c) body is a quaterrylene, the hydrophilic side chains are also negatively charged at basic pH. In this case, the $\pi-\pi$-stacking interactions should be optimized for the adsorption of **2** to the zigzag SWNT sidewalls. In both cases, starting from a raw mixture of SWNTs, the amphiphiles are expected to selectively solubilize in a basic aqueous medium some of the nanotubes: the armchair or close-to-armchair tubes using **1** and the zigzag or close-to-zigzag tubes using **2**.

A brief description of the optimized selection protocol is as follows. As-produced SWNTs were first submitted to a debundling procedure. HiPco SWNTs were dispersed in an aqueous SDS solution (1 wt %) by 1 h of low power sonication (20 W). The suspension was then ultracentrifuged at 130 000 × g for 1 h to pellet nanotube bundles and impurities. The supernatant was separated, leading to a SDS−micelle-suspended nanotube solution at a typical mass concentration from 20 to 25 mg L^{-1} (further centrifugation did not lead to the deposit of solid material).[26] The obtained suspension contained mainly individual SWNTs and SWNT bundles of a few nanotubes, all of which were covered with

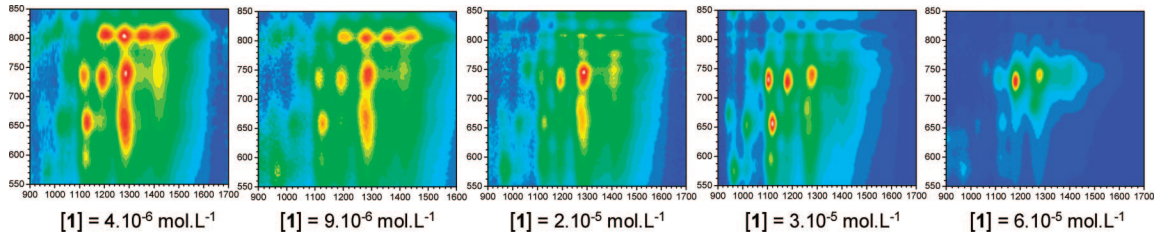

Figure 2. Photoluminescence spectra for the selection experiments of HiPco SWNTs by amphiphile **1**. The five spectra are contour plots of fluorescence intensity versus excitation (*Y* axis) and emission (*X* axis) wavelengths for samples of SWNTs suspended in deuterium oxide by the presence of compound **1** (the colours from blue to red indicate the strength of the emission). The experimental protocol is performed starting with various concentrations of **1**, indicated under each spectrum.

SDS.[26] To 1 mL of this sample was added 0.7 mL of an aqueous solution at various concentrations of amphiphile **1** or **2**. Then SDS was removed by extended dialysis, the remaining suspension was briefly sonicated and then centrifuged (1.5 h, 17 000 × g). At this stage, most of the SWNT material was in the pellet, but some nanotubes were maintained in the supernatant, which was separated. Most interestingly, control experiments in the absence of **1** and **2** showed that no SWNT remained in the supernatant at this stage. Thus, it appeared that, for the samples prepared in the presence of **1** or **2**, SWNTs contained in the supernatants corresponded to the fraction of the starting HiPco mixture that was maintained in solution thanks to the presence of the amphiphiles. Furthermore, we observed that the supernatant became darker gray in series of experiments where increasing quantities of amphiphiles were used, indicating that more SWNTs were solubilized.

The supernatants containing the solubilized nanotubes were then studied by two complementary techniques in order to analyze the (*n*,*m*) SWNT populations and to compare them with the starting HiPco sample: photoluminescence (PL) for the analysis of semiconducting tubes and resonant Raman spectroscopies (RRS) for the analysis of metallic tubes. The PL experiment consists in measuring the luminescence emission of the sample using excitation wavelengths in the range of 500−900 nm (by 3 nm steps). The result is a three-dimensional map showing absorption peaks characterized by precise excitation and emission wavelengths (Figure 2). Each peak can be assigned to a specific nanotube structure (*n*,*m*).[27] The PL experimental conditions used herein cover the whole distribution of the (*n*,*m*) semiconducting nanotubes in the HiPco material, but the metallic tubes contained in the samples are not seen by this technique.[28] In this respect, RRS is a complementary procedure, since it allows the relative quantification of the (*n*,*m*) population among the metallic SWNTs. Indeed, the radial breathing mode (RBM) section of the Raman spectra excited at precise wavelengths show peaks that can be precisely assigned to (*n*,*m*) metallic SWNTs.[29,30] For our samples, we used an excitation wavelength of 571.5 nm in order to scan the 24th (*n*,*m*) metallic family ($2n + m = 24$), which is the major metallic family of SWNTs contained in the HiPco material.

First will be described the PL analysis of the SWNTs selected by both amphiphiles **1** and **2**. For PL experiments, the aqueous supernatants obtained, containing the selected SWNTs, were dialyzed against D_2O in order to reach an H_2O content below 0.2%. The PL maps in Figure 2 were obtained from SWNT solutions prepared using increasing quantities of the pentacenic amphiphile **1**. At the lowest concentration studied, the selection protocol led to supernatants that were far diluted in SWNTs. Thus, the PL signals were very weak, moreover virtually no selection among the (*n*,*m*) population was noticeable (PL maps were very close to the starting HiPco material PL map, Figure 3a). This lack of selectivity might have been due to unfavorable competition with traces of SDS that would nonselectively disperse a small fraction of the material. Nevertheless, the use of **1** at higher concentrations led to remarkable changes in the PL maps (Figure 2). Indeed, at the highest concentration studied, the pentacenic amphiphile **1** mainly selected the tubes (8,6) and (8,7) (Figure 3b); as by comparison with the starting mixture (Figure 3a), the abundance of all other (*n*,*m*) tubes decreased (Figure 3b). As stated earlier, (*n*,*n*) armchair tubes can not be probed by PL for they are metallic. Hence, these results show that the semiconducting SWNTs that present a close-to-armchair structure (indices (*n*,*m*) such as *n* and *m* are close) were selected among all of the semiconducting tubes, by amphiphile **1** using our optimized selection protocol.

When amphiphile **2** was used instead of **1**, because of the low solubility and aggregation propensity of this quaterrylene derivative in water, the optimized selection protocol led only to much diluted SWNT solutions. Only the experiment conducted in the presence of **2** at the highest concentration (4×10^{-5} mol L^{-1}) led to a supernatant that could be accurately analyzed by PL spectroscopy. Even in this case, the PL signals were weak (Figure 3c). By analogy with experiments in the presence of **1** at low concentrations, we should have expected here that part of the PL signals was due to the nonselective dispersion of HiPco nanotubes by residual traces of SDS. Nevertheless, the PL map obtained after the SWNT selection by amphiphile **2** is substantially different from the maps obtained with the starting HiPco material (Figure 3a) or with the fraction of the material selected by compound **1** (Figure 3b), indicating that a selection among the SWNTs occurred and that this selection is different from the previously studied one. The comparison of the PL maps in Figure 3a,c shows that treatment by compound **2** led to the relative decrease of the close-to-armchair SWNT population ((7,6), (8,6), (8,7), (9,7)). An increase in the abundance is observed only for SWNTs which helicity angle is medium or low (between 0 and 15°: (9,4), (8,3), (10,2), (12,1)). It should be underlined that intrinsic

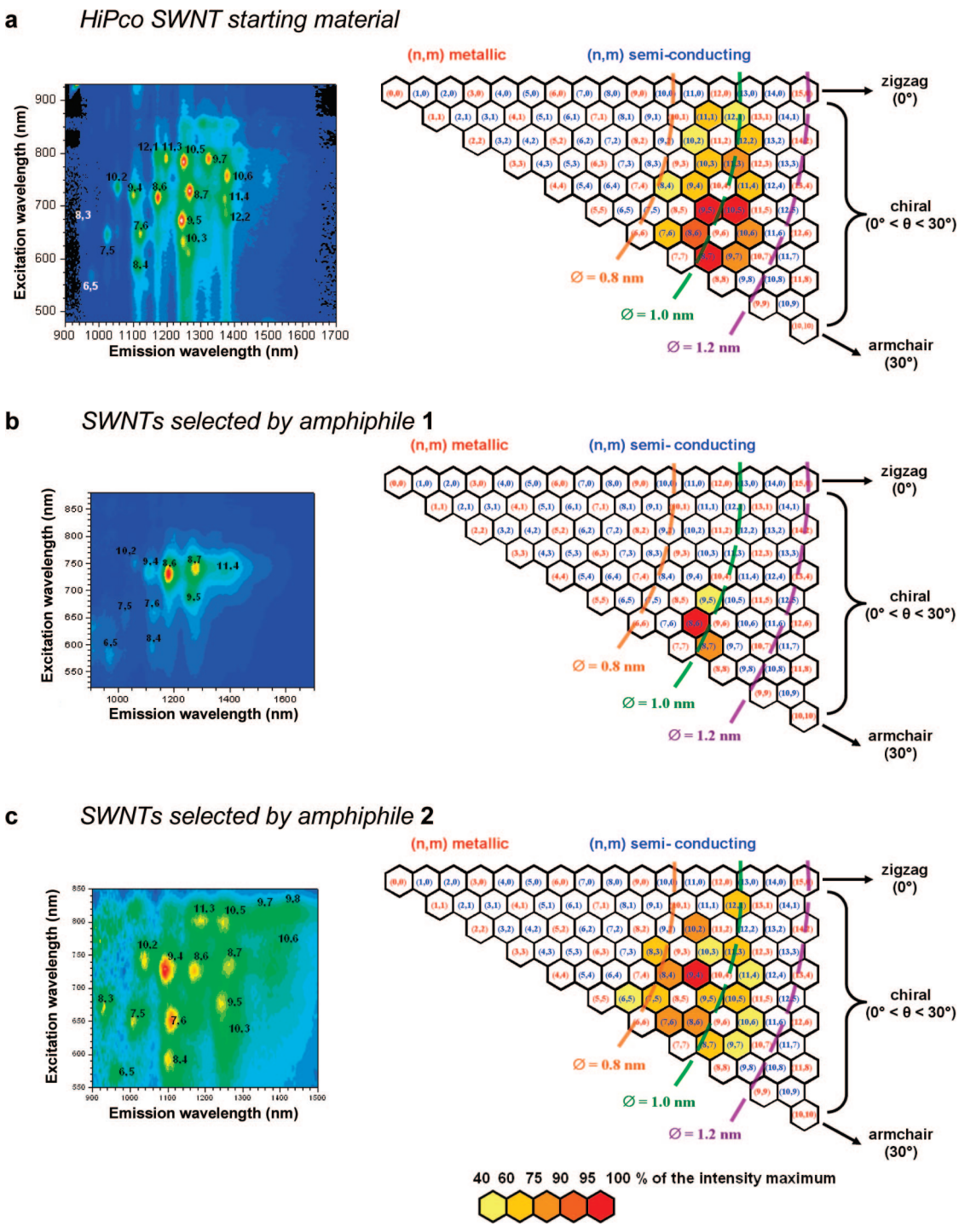

Figure 3. Photoluminescence spectra of the HiPco SWNT samples before and after the selection protocol. (a) PL intensity versus excitation and emission wavelengths for a HiPco SWNT sample suspended in SDS and deuterium oxide (the colours from blue to red indicate the strength of the emission). (b,c) Spectra of the extracted fractions of the previous HiPco SWNT sample using the reported selection protocol, and starting with amphiphile **1** at the concentration of 6×10^{-5} mol L^{-1} (b) or amphiphile **2** at the concentration of 4×10^{-5} mol L^{-1} (c). PL emissions intensities are reported on Hamada plots to illustrate the selections obtained.

PL for each (*n*,*m*) nanotube is expected to be very much dependent on the helicity angle. Specifically, it is considered that intrinsic PL decreases at low helicity angle and is nonexistent for semiconducting zigzag SWNTs.[31] For these reasons, even if zigzag nanotubes were to be selected by compound **2**, they could not be seen by PL spectroscopy, and an enrichment in close-to-zigzag nanotubes could lead to only low PL signals.

Thus, starting from the same dispersion of HiPco SWNTs, applying the same selection protocol, but using either amphiphile **1** or **2**, we observed by PL analysis the selection of two different subsets of nanotubes among the semiconducting ones. As predicted from the design of the amphiphiles, the use of **1** led to the selection of the large helicity angle population (armchair tubes), and the use of **2** led to the selection of the medium to low helicity angle

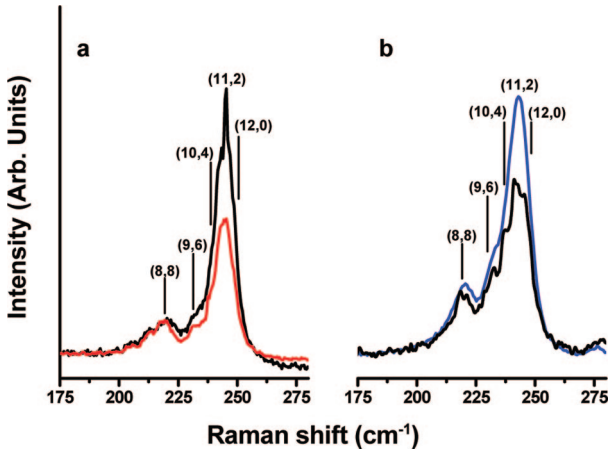

Figure 4. Resonant Raman spectroscopy of the HiPco SWNT samples before and after the selection protocol, for the probing of the 24th metallic SWNTs family (excitation at 571.5 nm). (a) The comparison of the spectra for the starting HiPco SWNTs (black) and for the fraction of SWNTs solubilized by **1** (red) show a decrease in the small helicity angle SWNT population: (10,4), (11,2), and (12,0). (b) The comparison of the spectra for the starting HiPco SWNTs (black) and for the fraction of SWNTs solubilized by **2** (blue) show an increase in the small helicity angle SWNT population: (11,2) and (12,0).

population (toward the zigzag tubes). To study a possible selection among the metallic SWNTs, RRS experiments were performed on the same samples as the ones presented in Figure 3b,c, and the results are presented below.

For RRS experiments the SWNTs yielded by the selection process were precipitated from the supernatants using an acidic treatment, and then the amphiphile (**1** or **2**) was removed from the tube sidewalls by several cycles of washes with slightly acidic water and methanol. Finally, the SWNT material was dried under vacuum. RRS was first used to probe whether the extraction protocol damaged the SWNTs sidewalls. The optimized separation protocol was proved to be quite smooth since the analysis of the RRS experiments in the tangential modes (TM) did not show any increase of the D-band assigned to SWNT defects in both of the samples obtained using **1** and **2** (data not shown). Then the 24th metallic SWNTs family population was analyzed by studying the radial breathing mode (RBM) section of the Raman spectra excited at 571.5 nm before and after the selection process in the presence of **1** or **2** (Figure 4). In order to avoid artifacts due to heterogeneity of the dried samples, three Raman spectra were recorded at different locations; only one representative spectrum is reported here. The spectra of the sample selected by **1** show a relative increase of the large helicity angle SWNT population (Figure 4a, (8,8), (9,6)) in the metallic family investigated compared with the starting material. Moreover the depletion in the selected SWNT population is all the more important as the helicity angle is small, namely, as SWNTs are closer to the zigzag structure (Figure 4a, (11,2), (12,0)). In considering now the RBM section of the Raman spectrum of the SWNT sample selected by **2**, it appears that in this case the small helicity angle SWNTs population has increased by comparison with the reference sample. Indeed the (12,0) zigzag or (11,2) close-to-zigzag over (8,8) armchair tube ratio is higher in the sample treated in the presence of **2** compared with the starting sample.

Thus, the RRS results on metallic tubes corroborate the ones obtained by PL on semiconducting tubes and prove that amphiphile **1** allowed the discrimination of SWNTs in favor of close-to-armchair and armchair tubes and that amphiphile **2** allowed the discrimination of SWNTs in favor of close-to-zigzag and zigzag tubes.

In summary, two aromatic amphiphiles were designed and synthesized for the selective solubilization of SWNTs according to their helicity angle. By using these molecules, a protocol was optimized for the sorting of HiPco SWNTs from a suspension in aqueous SDS. The carbon nanotubes selected by each of the two amphiphiles were of different helicities, demonstrating the specificity of the interactions between the amphiphiles and the carbon nanotubes. Our results are in agreement with the initial hypothesis, indicating that discriminations between SWNTs are possible thanks to the supramolecular recognition of the nanotube sidewall structure. The supramolecular recognition is mediated by the optimization of the $\pi-\pi$-stacking interactions between the polycyclic amphiphiles and the graphene lattice of armchair and zigzag nanotubes. These noncovalent interactions are reversible and leave the structure and the electronic properties of SWNTs unchanged. Our results give the proof of concept for new ways of tuning the selectivity of the sorting of SWNTs, possibly leading to samples with precise helicities. Hence, arising from the presented results, a separation protocol using optimized amphiphiles could complete the already existing sorting methods that allow the differentiation of SWNTs according either to their diameter or to their electronic properties. Particularly, the transposition of this strategy into a preparative method implies the synthesis of more soluble amphiphiles, especially for the selection of small helicity angle SWNTs population. The optimization of the procedure at a larger scale is ongoing in our laboratory in order to quantify the yield of the method.

Supporting Information Available: Protocols for the synthesis of amphiphiles **1** and **2**, for the separation of nanotubes are described as well as the PL and resonant Raman experiments. This material is available free of charge via the Internet at http://pubs.acs.org.

References

(1) Yuan, D.; Liu, J. *Small* **2007**, *3*, 366–367.
(2) Strano, M. S.; Dyke, C. A.; Usrey, M. L.; Barone, P. W.; Allen, M. J.; Shan, H.; Kittrell, C.; Hauge, R. H.; Tour, J. M.; Smalley, R. E. *Science* **2003**, *301*, 1519–1522.
(3) Maeda, Y.; Kimura, S.-I.; Kanda, M.; Hirashima, Y.; Hasegawa, T.; Wakahara, T.; Lian, Y.; Nakahodo, T.; Tsuchiya, T.; Akasaka, T.; Lu, J.; Zhang, X.; Gao, Y.; Yu, Y.; Nagase, S.; Kazaoui, S.; Minami, N.; Shimizu, T.; Tokumoto, H.; Saito, R. *J. Am. Chem. Soc.* **2005**, *127*, 10287–10290.
(4) Yudasaka, M.; Zhang, M.; Iijima, S. *Chem. Phys. Lett.* **2003**, *374*, 132–136.
(5) An, K. H.; Park, J. S.; Yang, C. M.; Jeong, S. Y.; Lim, S. C.; Kang, C.; Son, J. H.; Jeong, M. S.; Lee, H. Y. *J. Am. Chem. Soc.* **2005**, *127*, 5196–5203.
(6) Chen, Z. H.; Du, X.; Du, M. H.; Rancken, C. D.; Cheng, H. P.; Rinzler, A. G. *Nano Lett.* **2003**, *3*, 1245–1249.

(7) An, K. H.; Heo, J. G.; Jeon, K. G.; Bae, D. J.; Jo, C.; Yang, C. W.; Park, C. Y.; Lee, Y. H. *Appl. Phys. Lett.* **2002**, *80*, 4235–4237.
(8) Krupke, R.; Hennrich, F.; Loehneysen, H. V.; Kappes, M. M. *Science* **2003**, *301*, 344–347.
(9) Lee, D. S.; Kim, D. W.; Kim, H. S.; Lee, S. W.; Jhang, S. H.; Park, H. W.; Campbell, E. E. B. *Appl. Phys. A: Mater. Sci. Process.* **2005**, *80*, 5–8.
(10) Arnold, M. S.; Stupp, S. I.; Hersam, M. C. *Nano Lett.* **2005**, *5*, 713–718.
(11) Arnold, M. S.; Green, A. A.; Hulvat, J. F.; Stupp, S. I.; Hersam, M. C. *Nature Nanotech.* **2006**, *1*, 60–65.
(12) Choi, H. C.; Kim, W.; Wang, D.; Dai, H. *J. Phys. Chem. B* **2002**, *106*, 12361–12365.
(13) An, L.; Owens, J. M.; McNeil, L. E.; Liu, J. *J. Am. Chem. Soc.* **2002**, *124*, 13688–13689.
(14) He, M.; Ling, X.; Zhang, J.; Liu, Z. *J. Phys. Chem. B* **2005**, *109*, 10946–10951.
(15) Zheng, M.; Jagota, A.; Strano, M. S.; Santos, A. P.; Barone, P.; Chou, S. G.; Diner, B. A.; Dresselhaus, M. S.; Mclean, R. S.; Onoa, G. B.; Samsonidze, G. G.; Semke, E. D.; Usrey, M.; Walls, D. J. *Science* **2003**, *302*, 1545–1548.
(16) Zheng, M.; Jagota, A.; Semke, E. D.; Diner, B. A.; Mclean, R. S.; Lustig, S. R.; Richardson, R. E.; Tassi, N. G. *Nat. Mater.* **2003**, *2*, 338–342.
(17) Strano, M. S.; Zheng, M.; Jagota, A.; Onoa, G. B.; Heller, D. A.; Barone, P. W.; Usrey, M. L. *Nano Lett.* **2004**, *4*, 543–550.
(18) Shigeta, M.; Komatsu, M.; Nakashima, N. *Chem. Phys. Lett.* **2006**, *418*, 115–118.
(19) Nish, A.; Hwang, J.-Y.; Doig, J.; Nicholas, R. J. *Nature Nanotech.* **2007**, *2*, 640–246.
(20) Chen, F.; Wang, B.; Chen, Y.; Li, L.-J. *Nano Lett.* **2007**, *7*, 3013–3017.
(21) Peng, X.; Komatsu, N.; Bhattacharya, S.; Shimawaki, T.; Aonuma, J.; Kimura, T.; Osuka, A. *Nature Nanotech.* **2007**, *2*, 361–365.
(22) Peng, X.; Komatsu, N.; Kimura, K.; Osuka, A. *J. Am. Chem. Soc.* **2007**, *129*, 15947–15953.
(23) Gotovac, S.; Honda, H.; Hattori, Y.; Takahashi, K.; Kanoh, H.; Kaneko, K. *Nano Lett.* **2007**, *7*, 583–587.
(24) Tournus, F.; Latil, S.; Heggie, M. I.; Charlier, J.-C. *Phys. Chem. Rev. B* **2005**, *72*, 075431.
(25) Lu, J.; Nagase, S.; Zhang, X.; Wang, D.; Ni, M.; Maeda, Y.; Wakahara, T.; Nakahodo, T.; Tsuchiya, T.; Akasaka, T.; Gao, Z.; Yu, D.; Ye, H.; Mei, W. N.; Zhou, Y. *J. Am. Chem. Soc.* **2006**, *128*, 5114–5118.
(26) O'Connell, M. J.; Bachilo, S. M.; Huffman, C. B.; Moore, V. C.; Strano, M. S.; Haroz, E. H.; Rialon, K. L.; Boul, P. J.; Noon, W. H.; Kittrell, C.; Ma, J.; Hauge, R. H.; Weisman, R. B.; Smalley, R. E. *Science* **2002**, *297*, 593–596.
(27) Bachilo, S. M.; Strano, M. S.; Kittrell, C.; Hauge, R. H.; Smalley, R. E.; Weisman, R. B. *Science* **2002**, *298*, 2361–2366.
(28) Lebedkin, S.; Arnold, K.; Hennrich, F.; Krupke, R.; Renker, B.; Kappes, M. M. *New J. Phys.* **2003**, *5*, 140.
(29) Wiltshire, J. G.; Li, L.-J.; Herz, L. M.; Nicholas, R. J.; Glerup, M.; Sauvajol, J.-L.; Khlobystov, A. N. *Phys. Rev. B* **2005**, *72*, 205431.
(30) Strano, M. S.; Doorn, S. K.; Haroz, E. H.; Kittrell, C.; Hauge, R. H.; Smalley, R. E. *Nano Lett.* **2003**, *3*, 1091–1096.
(31) Oyama, Y.; Saito, R.; Sato, K.; Jiang, J.; Samsonidze, G. G.; Gruneis, A.; Miyauchi, Y.; Maryama, S.; Jorio, A.; Dresselhaus, G.; Dresselhaus, M. S. *Carbon* **2006**, *44*, 873–879.

NL0803141